Afyon Kocatepe Üniversitesi Fen ve Mühendislik Bilimleri Dergisi
Afyon Kocatepe University – Journal of Science and Engineering
https://dergipark.org.tr/tr/pub/akufemubid

Araştırma Makalesi / Research Article
e-ISSN: 2149-3367
DOI: https://doi.org/10.35414/akufemubid.1929318
CITE: Afyon Kocatepe University Journal of Science and Engineering. **26(4)** (2026) 954-963

Investigation of the Combined Effect of Sandblasting Pressure and Angle on the Surface Characteristics of Titanium for Dental Implant Applications

Makale Bilgisi / Article Info
Alındı/Received: 13.04.2026
Kabul/Accepted: 06.07.2026
Yayımlandı/Published: 03.08.2026

Diş İmplantı Uygulamaları İçin Titanyumun Yüzey Özellikleri Üzerine Kumlama Basıncı ve Açısının Birleşik Etkisinin İncelenmesi

Ozan YILMAZ*

Dokuz Eylul University, Faculty of Engineering, Department of Metallurgical and Materials Engineering, Izmir, Türkiye

Abstract

In this study, titanium surfaces used as dental implant materials were modified under different grit blasting pressures (2, 4, and 6 bar) and blasting angles (30°, 60°, and 90°). Al_2O_3 particles with a median particle size of D_{50} = 100 µm were used as the abrasive medium during the grit blasting process. The surface morphologies of the produced samples were examined by scanning electron microscopy (SEM), their phase structures were determined by X-ray diffraction (XRD), and their surface topographies were analyzed using a profilometer. In addition, surface wettability was evaluated by contact angle measurements using distilled water. The results showed that increasing the grit blasting pressure and applying the blasting angle more perpendicular to the surface markedly increased surface roughness and microtopographic complexity. The highest arithmetical mean height (S_a) value was obtained under the 6 bar 90° (B6-A90) condition as 2.58 µm, corresponding to an approximately 200% increase compared with the untreated titanium surface, which exhibited an S_a value of 0.86 µm. Contact angle measurements revealed that the lowest value was obtained for the 4 bar 90° (B4-A90) sample as 69.11°, which was approximately 23.4% lower than that of the 6 bar 30° (B6-A30) sample showing the highest contact angle. Overall, the B6-A90 condition was evaluated as the most suitable surface modification parameter for dental implant applications because it provided a combined balance of high surface roughness, complex microcrater formation, and hydrophilic behavior.

Keywords: *Titanium; Sandblasting; Surface Roughness; Contact Angle; Dental Implant; Surface Characterization.*

Öz

Bu çalışmada, dental implant malzemesi olarak kullanılan titanyum yüzeyler, farklı kumlama basınçları (2, 4 ve 6 bar) ve kumlama açıları (30°, 60° ve 90°) altında modifiye edilmiştir. Kumlama işlemlerinde aşındırıcı olarak ortalama partikül boyutu D_{50} = 100 µm olan Al_2O_3 partikülleri kullanılmıştır. Üretilen numunelerin yüzey morfolojileri taramalı elektron mikroskobu (SEM) ile incelenmiş, faz yapıları X-ışını difraksiyonu (XRD) yöntemiyle belirlenmiş ve yüzey topografyaları profilometre ile analiz edilmiştir. Ayrıca, yüzey ıslanabilirliği, saf su kullanılarak gerçekleştirilen temas açısı ölçümleriyle değerlendirilmiştir. Elde edilen sonuçlar, kumlama basıncındaki artışın ve kumlama açısının yüzeye daha dik hâle gelmesinin yüzey pürüzlülüğünü ve mikrotopografik karmaşıklığı belirgin şekilde artırdığını göstermiştir. En yüksek aritmetik ortalama yüzey pürüzlülüğü (S_a) değeri 6 bar 90° (B6-A90) koşulunda 2.58 µm olarak elde edilmiş ve bu değer işlem görmemiş titanyum yüzeyine ait 0.86 µm değerine göre yaklaşık %200 artış göstermiştir. Temas açısı ölçümlerinde en düşük değer 4 bar 90° (B4-A90) numunesinde 69.11° olarak belirlenmiş ve bu değer en yüksek temas açısına sahip 6 bar 30° (B6-A30) numunesine göre yaklaşık %23.4 daha düşük bulunmuştur. Genel olarak, B6-A90 koşulu; yüksek yüzey pürüzlülüğü, kompleks mikrokrater oluşumu ve hidrofilik davranışın birlikte sağlanması bakımından dental implant yüzey modifikasyonu için en uygun işlem parametresi olarak değerlendirilmiştir.

Anahtar Kelimeler: *Titanyum; Kumlama; Yüzey Pürüzlülüğü; Temas Açısı; Dental İmplant; Yüzey Karakterizasyonu.*

1. Introduction

Dental implants have become the gold standard in modern dentistry for the functional and aesthetic rehabilitation of missing teeth. In these applications, titanium (Ti) and its alloys are accepted as "gold standard" materials due to their low elastic modulus, high corrosion resistance, and excellent biocompatibility (Ban et al., 2006, Gil et al., 2007, Chrcanovic et al., 2016). The biological success of titanium relies on the interaction between the thin, stable oxide layer (TiO2) that forms spontaneously on its surface and the surrounding tissues.

However, since titanium has a biologically inert structure, it may be difficult to establish a rapid integration with the bone tissue after implantation (Khan et al., 2016, Sykaras et al., 2000). In this context, the osseointegration process, which is the most fundamental criterion for implant success, is defined as the establishment of a functional connection between the implant surface and the alveolar

*Sorumlu Yazar/Corresponding Author: Ozan YILMAZ
e-posta/e-mail: ozan.yilmaz@deu.edu.tr

bone (Sykaras et al., 2000). The success of osseointegration depends on the material's biocompatibility, its design, the surgical technique, and, most importantly, the implant's surface characteristics. In the literature, it has been determined that surface roughness and chemical composition have a direct effect on the proliferation and differentiation of bone cells (osteoblasts)(Sykaras et al., 2000, Rønold et al., 2003). It is known that rough surfaces, compared to smooth surfaces, increase protein adsorption and accelerate blood platelet activation by providing a larger effective surface area. To improve this mechanism, various surface modification methods, such as sandblasting, acid etching, anodizing, and plasma spraying, have been developed (Ban et al., 2006, Anbarzadeh and Mohammadi, 2023, Thakur et al., 2022).

The sandblasting method, based on striking hard abrasive particles onto the surface with compressed air, is one of the most frequently used techniques for creating macro-roughness on dental implants. In this process, aluminum oxide (Al_2O_3), silicon oxide (SiO_2), or titanium oxide (TiO_2) particles are generally used(Ghara et al., 2021). The surface topography obtained by sandblasting depends directly on particle size, blasting pressure, distance, and impact angle (Ghara et al., 2021). As surface roughness (Ra) increases, the removal torque of the implant increases, and mechanical interlocking is strengthened (Elias et al., 2008). Similarly, it has been found that acid-etching processes applied after sandblasting maximize the osseointegration potential by increasing surface microporosity (Akbas et al., 2025).

In addition to the physical structure of the surface, wettability is also a critical parameter for biological interactions (Gittens et al., 2014). Hydrophilic surfaces support the bone-healing process by facilitating the spread of biological fluids on the surface. The positive effects of hydrophilic surfaces on early-stage bone attachment(Rupp et al., 2006). Optimization of sandblasting parameters can ensure achieving ideal roughness values and obtaining super-hydrophilic characteristics by increasing surface energy (Rupp et al., 2006). Although there are numerous studies in the current literature on the effect of sandblasting pressure on roughness, systematic investigations into the combined effects of sandblasting angle together with pressure on surface morphology and wettability are observed to be limited (Kırman et al., 2023, Akbas et al., 2025). Especially in ductile materials such as Grade 2 commercially pure titanium, the impact angle's effect on particle penetration and surface deformation is a key factor in topographic optimization.

The aim of this study is to comprehensively investigate the effects of sandblasting pressure (2, 4, and 6 bar) and sandblasting angle (30°, 60°, and 90°) on the surface characteristics of titanium surfaces used as dental implant materials. Within the scope of the study, the effects of different parameter combinations on average surface roughness (Ra), surface morphology (SEM), phase structure (XRD), and wettability are determined, aiming to identify the most favorable surface preparation conditions for biological performance.

2. Materials and Methods

2.1. Sample Preparation

In this study, Grade 2 titanium (Ti) discs with a diameter of 10 mm and a thickness of 3 mm, possessing suitable properties for dental implant applications, were used. To ensure standardization of the initial surface roughness prior to sandblasting, the sample surfaces were mechanically ground using SiC-based abrasive papers with mesh sizes of 400, 600, 800, 1000, and 1200, respectively. Following the grinding process, the samples were ultrasonically cleaned in ethanol, acetone, and distilled water for 10 minutes at each stage to completely remove metallic residues and potential surface oils. After the cleaning stage, all samples were dried under compressed air at room temperature.

2.2. Sandblasting Process and Experimental Design

Surface modification processes were performed using a Reitel Sanduret 2K (Reitel, Germany) model sandblasting device, a standard in dental laboratory applications. The experimental setup and the internal configuration of the sandblasting chamber are illustrated in Figure 1.

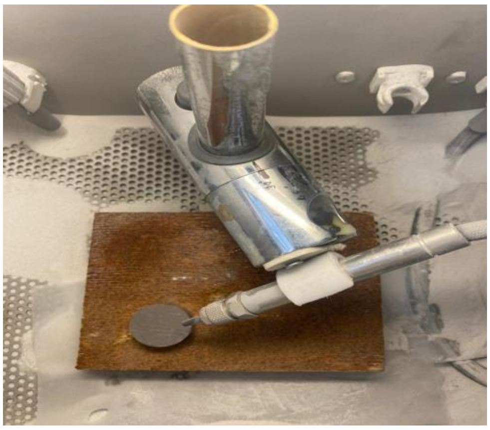

Figure 1. Detailed view of the experimental sandblasting setup and the surface modification process.

The figure demonstrates the internal working environment of the abrasive chamber, where the titanium sample is precisely positioned relative to the blasting nozzle tip. The setup was designed to ensure a constant blasting distance of 10 mm between the nozzle and the titanium surface. As shown in the visual, the abrasive particles were projected through a specialized nozzle within a sealed chamber, ensuring uniform distribution of kinetic energy across the target area. This configuration enabled the systematic adjustment of the blasting angle (30°, 60°, or 90°) and pressure (2, 4, or 6 bar) to effectively modify the surface topography. Angular aluminum oxide (Al_2O_3) particles with a median particle size of D50 = 100 µm were used as the abrasive medium. For all experimental conditions, the blasting distance was kept constant at 10 mm and the processing duration was fixed at 1 min. This constant processing time was used for all samples to isolate the effects of pressure and angle on surface morphology, roughness, and wettability.

After sandblasting, all samples were recleaned in an ultrasonic bath for 10 minutes to remove loosely attached abrasive residues. The primary experimental parameters are summarized in Table 1, and the specific sample identification codes are presented in Table 2.

Table 1. Experimental parameters for the sandblasting process.

Parameter	Value / Description
Abrasive Material	Aluminum Oxide (Al_2O_3)
Particle size	D50 = 100 µm
Blasting Pressures	2 bar, 4 bar, 6 bar
Blasting Angles	30^o,60^o,90^o
Blasting Distance	10 mm (Constant)
Processing Duration	1 minute (Constant)
Surface Cleaning Method	Ultrasonic Bath (Ethanol, Acetone, Distilled Water)

Table 2. Sample identification codes and parameters. In the sample codes, "B" represents the blasting pressure and "A" represents the blasting angle.

Sample Code	Pressure (bar)	Angle (°)
B2-A30	2	30
B2-A60	2	60
B2-A90	2	90
B4-A30	4	30
B4-A60	4	60
B4-A90	4	90
B6-A30	6	30
B6-A60	6	60
B6-A90	6	90
Pure Ti	0	0

2.3. Surface Characterization Techniques

To determine the topographic changes of the modified surfaces, average surface roughness (Ra) values were measured using a Surftest SJ-301 (Mitutoyo, Japan) profilometer. Measurements were taken from three different directions on the surface of each sample, and the average of these values was reported. The surface morphology and particle-surface interaction were analyzed using a Carl Zeiss 300VP model Scanning Electron Microscope (SEM). The crystal structures of the particles were determined using a Rigaku ULTIMA 3-Rint 2200/PC X-ray diffractometer (XRD) in the 2h range of 3–90 o, with Cu Ka radiation (0.1542 nm) at 40 kV and 36 mA. The wettability properties of the samples were evaluated by contact angle measurements using distilled water at room temperature. During the measurement, a distilled water droplet was placed on the sample surface, and the angle formed between the droplet and the surface was recorded using a contact angle measurement system. The obtained contact angle values were used to classify the surface behavior as hydrophilic or hydrophobic. Micro-Vickers hardness measurements were also performed on the untreated and grit-blasted titanium surfaces to evaluate the near-surface hardening effect induced by particle impact. The measurements were carried out under a load of 1 kgf and reported as HV_1. Representative hardness values were calculated from stable indentation measurements; non-representative indentations affected by local peaks, crater edges, or inclined roughness features were excluded from the final evaluation.

3. Results and Discussions

3.1. XRD analysis

The XRD patterns of untreated titanium (Pure Ti) and titanium samples sandblasted under different pressure and angle combinations are presented in Figure 2. For all samples, the major diffraction peaks observed at approximately 2θ = 35.1°, 38.4°, 40.2°, 53.0°, 62.9°, 70.6°, 76.2°, and 77.4° correspond to the (100), (002), (101), (102), (110), (103), (112), and (201) planes of the hexagonal close-packed (HCP) α-Ti phase, respectively (JCPDS Card No: 44-1294) (Low et al., 2019). These results indicate that the fundamental crystal structure of titanium was preserved after the sandblasting treatment.

No additional peaks associated with newly formed phases were detected in the XRD patterns after grit blasting. In particular, the absence of distinct diffraction peaks related to titanium oxide phases or residual Al_2O_3 particles used as the abrasive medium suggests that the applied surface treatment did not alter the phase constitution of the material and did not leave crystallographically detectable residues on the surface.

However, when the untreated Pure Ti sample is compared with the grit-blasted specimens, slight reductions in peak intensity and limited peak broadening can be observed for some reflections. This behavior may be attributed to the high-velocity impact of Al_2O_3 particles on the titanium surface, which can induce plastic deformation, lattice distortion, and residual stress in the surface and near-surface regions.

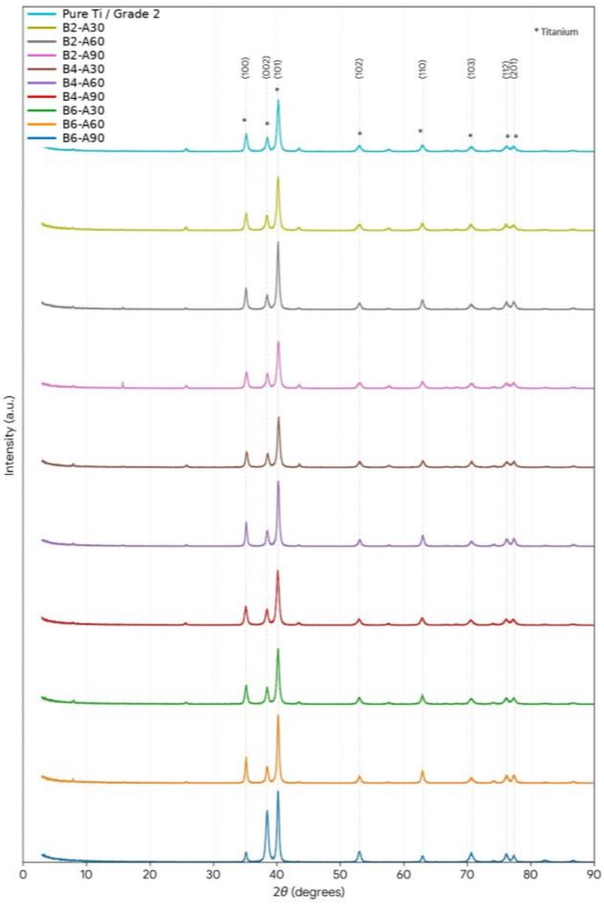

Figure 2. XRD patterns of untreated titanium (Pure Ti, Grade 2) and titanium samples sandblasted under different pressures (2, 4, and 6 bar) and angles (30°, 60°, and 90°) conditions.

This interpretation is further supported by the micro-Vickers hardness results presented in Section 3.5, where all grit-blasted surfaces exhibited higher hardness values than Pure Ti and the highest hardness value was obtained for B6-A90. Nevertheless, since no significant peak shift or phase transformation was observed, these changes are mainly attributed to microstructural disorder confined to the near-surface region.

Overall, the XRD results demonstrate that the grit blasting process did not impair the phase stability of titanium, but rather introduced deformation-related microstructural modifications in the surface and subsurface regions. These changes are directly associated with the variations in surface roughness, wettability, morphology, and hardness discussed in the following sections.

3.2. Surface Morphology (SEM Analysis)

The effects of sandblasting parameters on the titanium surface topography were investigated at different magnifications (500x and 5000x), and the recorded SEM images are presented between Figure 3 and Figure 8. The morphological examinations revealed that the sandblasting pressure and angle shaped the surface modification through "plowing" and "impact" mechanisms.

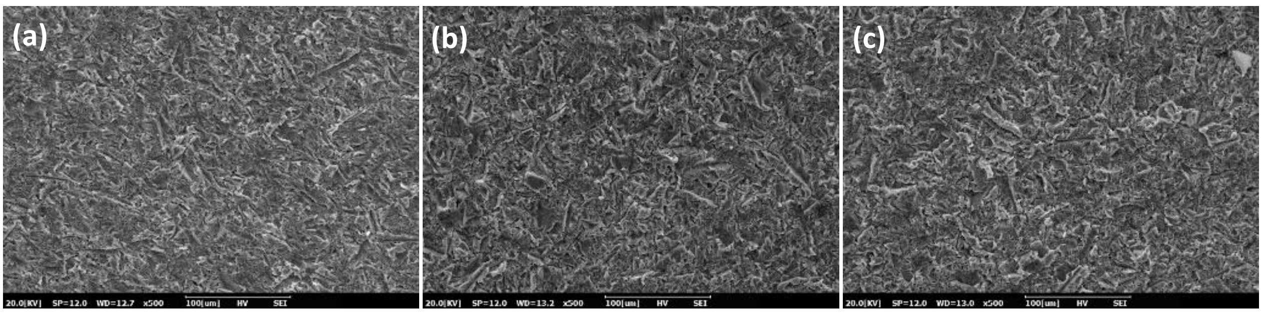

Figure 3. SEM images of a) B2-A30, b) B2-A60, and c) B2-A90 samples prepared under 2 bar constant pressure (500×). Scale bars are indicated in the micrographs

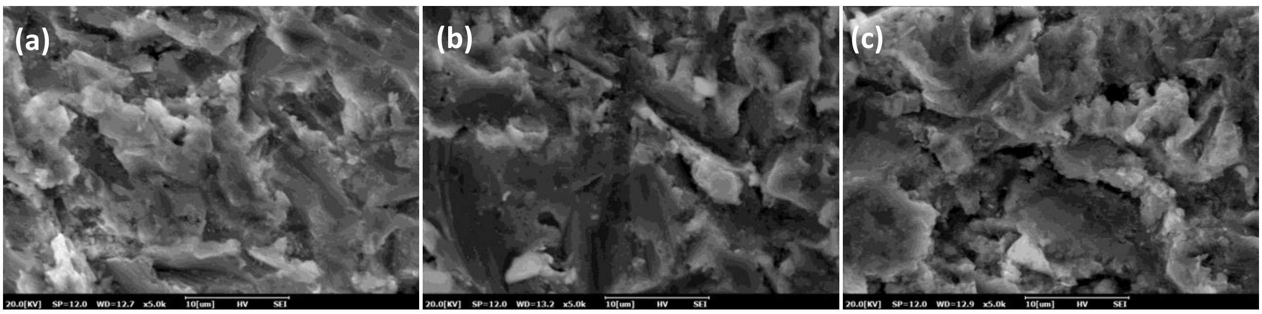

Figure 4. High-resolution SEM images of a) B2-A30, b) B2-A60, and c) B2-A90 samples prepared under 2 bar constant pressure (5000×).

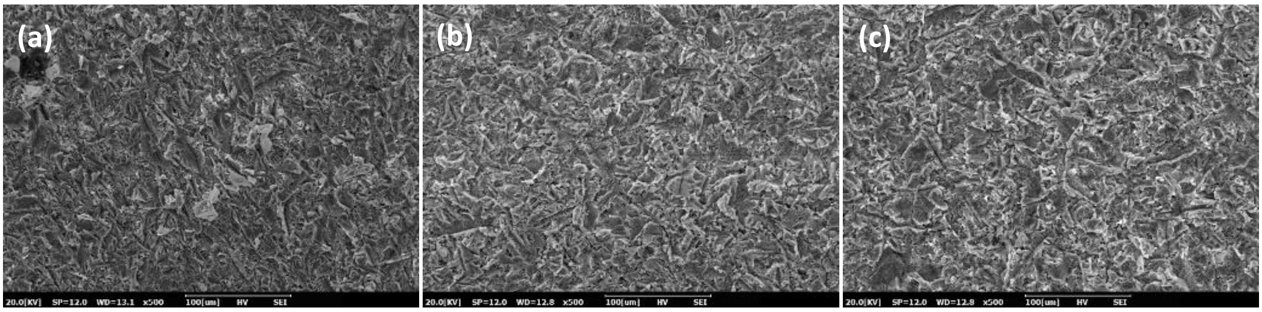

Figure 5. SEM images of a) B4-A30, b) B4-A60, and c) B4-A90 samples prepared under 4 bar constant pressure (500×).

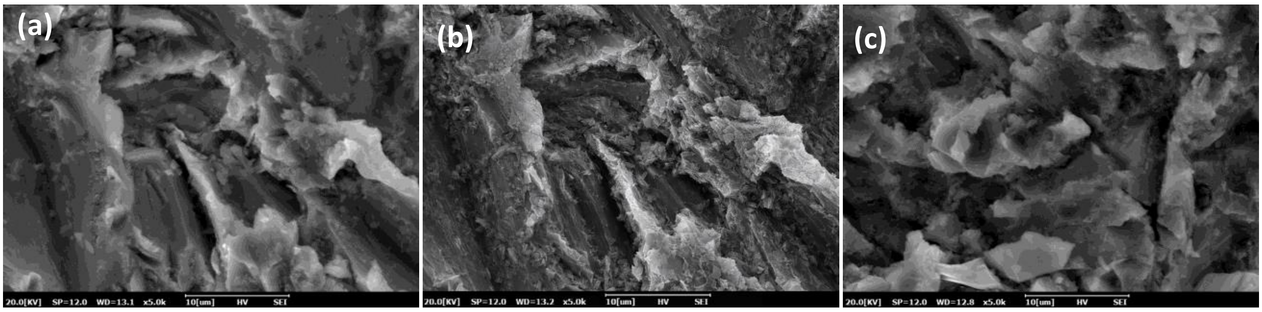

Figure 6. High-resolution SEM images of a) B4-A30, b) B4-A60, and c) B4-A90 samples prepared under 4 bar constant pressure (5000×).

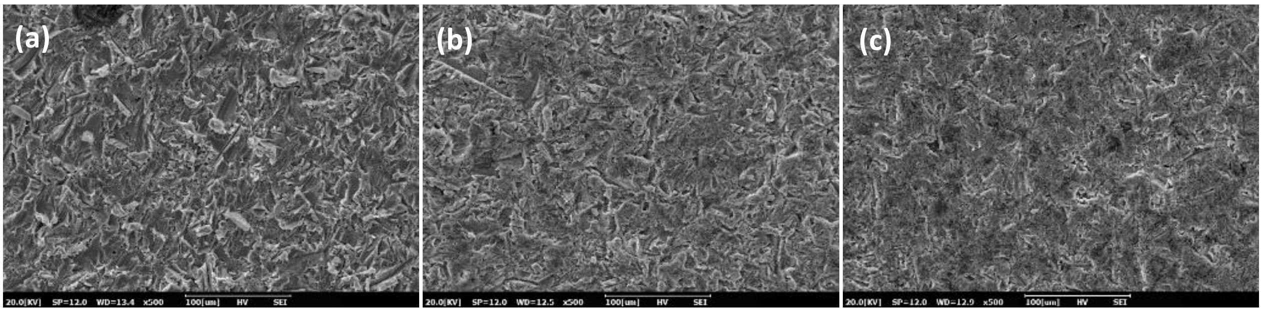

Figure 7. SEM images of a) B6-A30, b) B6-A60, and c) B6-A90 samples prepared under 6 bar constant pressure (500×).

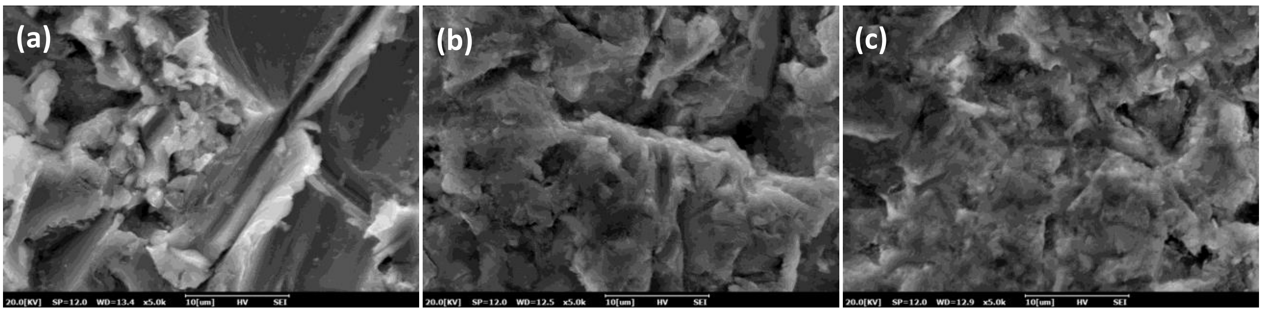

Figure 8. High-resolution SEM images of a) B6-A30, b) B6-A60, and c) B6-A90 samples prepared under 6 bar constant pressure (5000×).

In treatments performed under a constant pressure of 2 bar, the particles mainly skimmed the surface, leading to the formation of shallow micro-channels, especially at the low blasting angle in B2-A30 (Fig. 3.a). High-resolution images at 5000× magnification (Fig. 4.) indicated that this low-energy contact induced limited plastic flow on the ductile titanium surface, leaving a micro-texture with smoother transitions. With the increase in blasting angle to 90° in B2-A90 (Fig. 3.c), circular micro-depressions began to form as a result of more perpendicular particle impact; however, the severity of deformation remained limited due to the low pressure. Increasing the blasting pressure to 4 bar enhanced the depth and complexity of crater-like surface features due to the increase in kinetic energy (Fig. 5). In B4-A90 (Fig.5.c. and Fig. 6.c.), overlapping micro-craters formed a more complex morphology compared with the 2 bar group. This finding is consistent with the literature reporting that increasing blasting pressure increases the extent of surface deformation and roughness (Elias et al., 2008). The most pronounced morphological changes were recorded under the highest pressure of 6 bar (Fig. 7). Particularly for B6-A90 (Fig. 7c and Fig. 8c), a highly complex micro-topography consisting of crater-like depressions and sharp-edged features was obtained. Such a micro-architecture can promote mechanical interlocking and facilitate early biological attachment processes by providing a larger and more complex surface area (Le Guéhennec et al., 2007). Overall, increasing the blasting angle transformed the dominant wear mode from plowing toward direct impact, while increasing pressure intensified the deformation response. The combination of high roughness, complex microcrater morphology, hydrophilic behavior, and increased hardness supports the selection of B6-A90 as the most favorable overall surface modification condition in this study.

3.3. Surface Roughness and Topographic Analysis

The quantitative impact of sandblasting pressure and angle on the titanium surface architecture was evaluated using areal profilometry over a 1 × 1 mm scan area, with the results detailed in Table 3. The three-dimensional (3D) topographic maps presented in Figure 9. correlate the textural anisotropy and peak-to-depression distribution with the quantitative roughness parameters.

Table 3. Surface roughness parameters of titanium samples modified at different sandblasting pressures and angles.

Map label	Parameter	Sa (µm)	Sq (µm)	St (µm)	Sp (µm)	Sv (µm)
a	B2-A30	1.72	2.07	12.61	7.43	5.18
b	B2-A60	1.68	2.01	12.41	6.57	5.84
c	B2-A90	1.03	1.28	10.31	5.22	5.10
d	B4-A30	2.03	2.44	15.83	7.47	8.36
e	B4-A60	1.29	1.61	14.13	5.93	8.21
f	B4-A90	1.04	1.38	21.59	8.04	13.54
g	B6-A30	1.97	2.47	20.67	11.73	8.93
h	B6-A60	1.43	1.89	29.69	19.13	10.56
i	B6-A90	2.58	3.09	17.91	8.93	8.98
j	Pure Ti	0.86	1.08	7.38	4.01	3.37

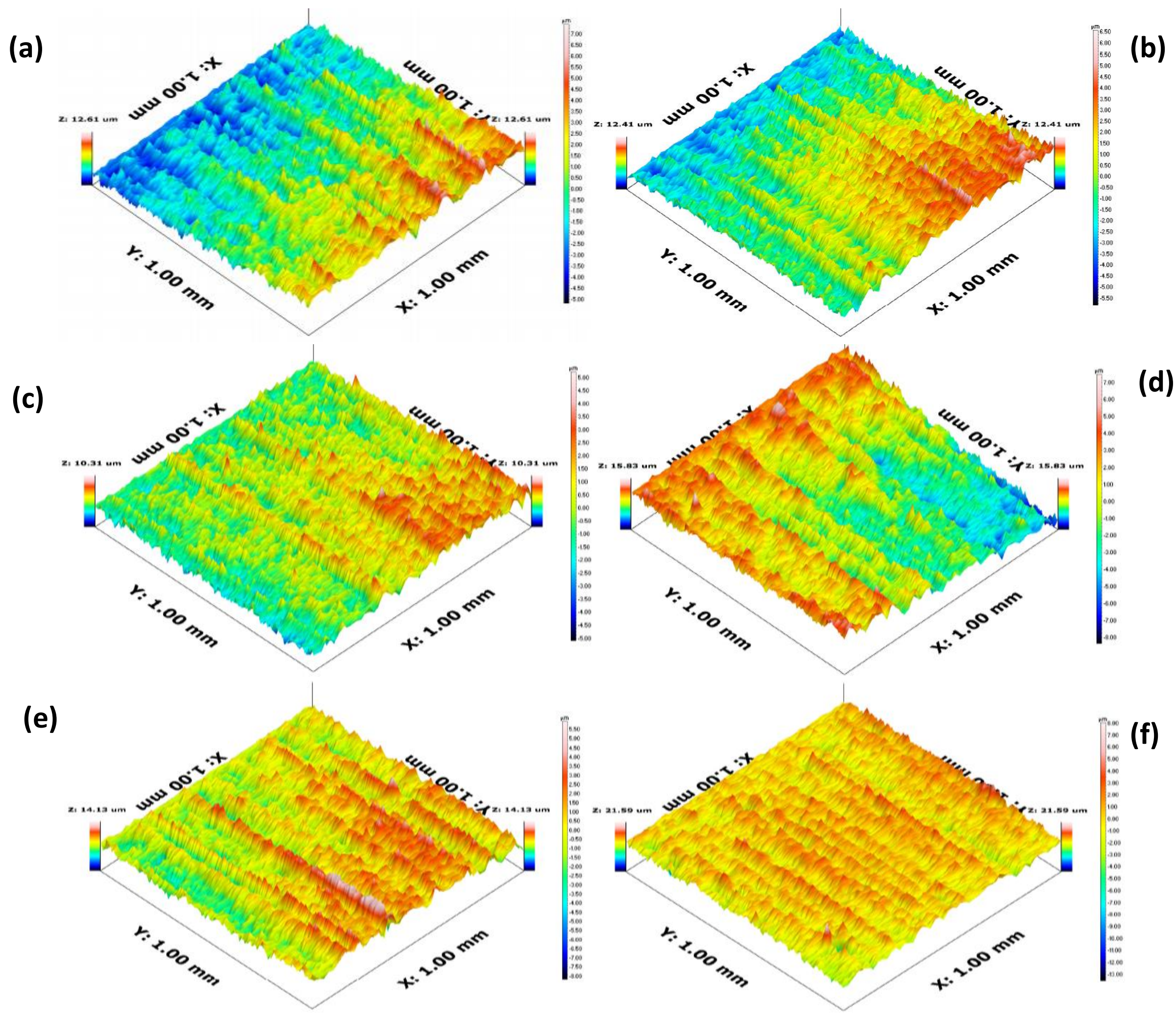

Figure 9. Three-dimensional (3D) topographic maps and surface roughness parameters of titanium surfaces modified under different sandblasting pressure and angle conditions: (a) B2-A30, (b) B2-A60, (c) B2-A90, (d) B4-A30, (e) B4-A60, (f) B4-A90, (g) B6-A30, (h) B6-A60, (i) B6-A90, and (j) untreated Pure Ti control sample.

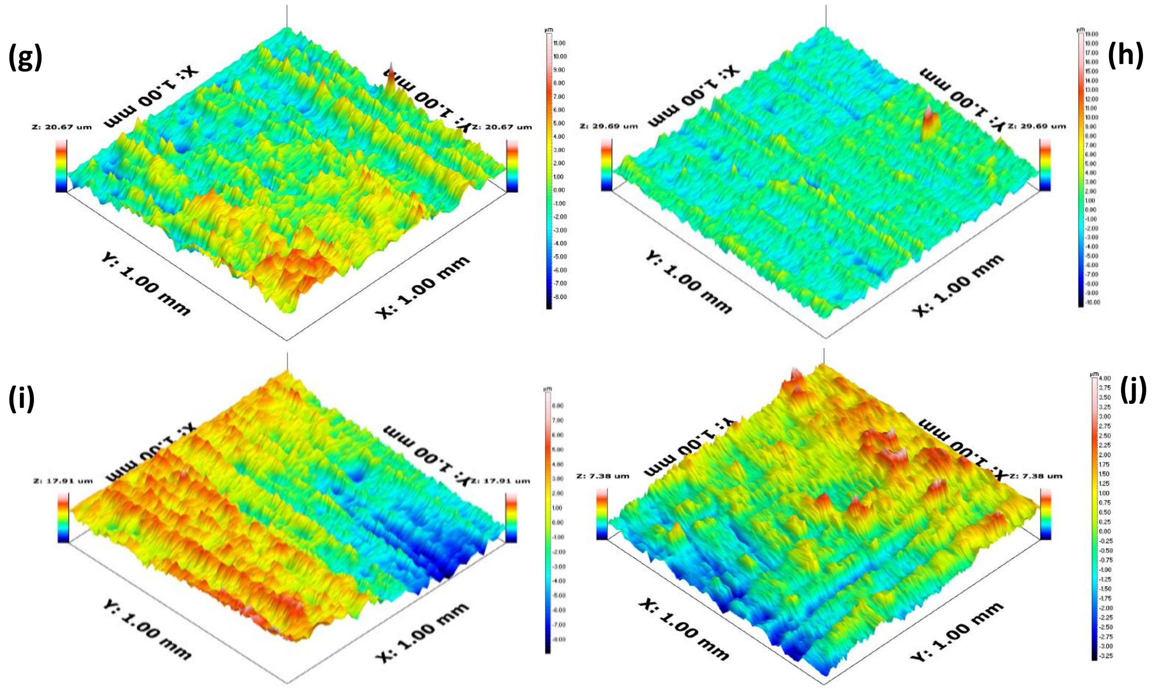

Figure 9 (continued). Three-dimensional (3D) topographic maps and surface roughness parameters of titanium surfaces modified under different sandblasting pressure and angle conditions: (a) B2-A30, (b) B2-A60, (c) B2-A90, (d) B4-A30, (e) B4-A60, (f) B4-A90, (g) B6-A30, (h) B6-A60, (i) B6-A90, and (j) untreated Pure Ti control sample.

Analysis of the topographic maps in Figure 9 reveals that the relatively smooth surface of the Pure Ti sample was transformed into a higher-frequency topography after sandblasting. Among the areal roughness parameters, Sa represents the arithmetical mean height of the surface, Sq denotes the root mean square height, St corresponds to the total height of the surface, Sp indicates the maximum peak height, and Sv represents the maximum depth of surface depressions (Sushil et al., 2025; Webb et al., 2012). Therefore, Sp and Sv provide complementary information on the peak-like protrusions and crater-like depressions generated by sandblasting.

The increase in Sa observed in B2-A30 and B4-A30 is mainly related to the linear heterogeneity created by plowing channels formed during oblique particle impact. In contrast, B6-A90 exhibited a more isotropic topography consisting of randomly distributed microcraters without a dominant directionality. The high correlation between Sa and Sq values indicates a relatively homogeneous distribution of surface height variations. B6-A90 exhibited the highest roughness value of the series, with an Sa value of 2.58 µm, representing an approximately 200% increase compared with untreated Pure Ti (0.86 µm).

When examining St (total profile height), a volumetric indicator, the value of 29.69 µm for the B6-A60 (h) sample is particularly noteworthy. This high amplitude confirms the presence of micron-scale peaks (Sp: 19.13 µm) generated by the impacts of the blasting media, which act as mechanical anchors in biological environments, contributing to peri-implant tissue integration (Le Guéhennec et al., 2007).

The relatively high Sv value of 13.54 µm detected in B4-A90 indicates the formation of deep crater-like surface depressions. These local depressions may contribute to liquid retention and help explain the low contact angle measured for this sample. Thus, the wettability behavior should be evaluated not only in terms of average roughness but also considering the local crater geometry, peak distribution, and surface depression characteristics.

3.4. Wettability Analysis

The effects of sandblasting parameters on the wettability behavior of titanium surfaces were evaluated by contact angle measurements using distilled water. Representative water droplet images obtained from selected samples are presented in Figure 10 to visually support the contact angle values listed in Table 4. The selected images include B2-A90, B4-A90, and B6-A30, representing different wettability responses observed in the study. The B2-A90 sample exhibited hydrophilic behavior with a contact angle of 71.68°, while B4-A90 showed the lowest contact angle value of 69.11°, corresponding to the highest wettability among the tested conditions. In contrast, B6-A30 exhibited a contact angle of 90.17°, indicating a borderline hydrophobic response.

The contact angle results show that most of the sandblasted titanium surfaces exhibited hydrophilic behavior, with contact angle values below 90°. However, the wettability variation was not strictly linear with sandblasting pressure or angle. This indicates that wettability was not governed solely by the average surface roughness value, but was also influenced by crater-like surface morphology, local liquid retention, surface depressions, and plowing-induced surface features.

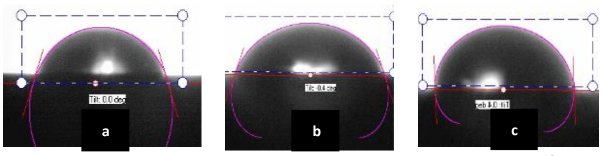

Figure 10. Representative water droplet images obtained from selected sandblasted titanium surfaces: (a) B2-A90, showing hydrophilic behavior with a contact angle of 71.68°; (b) B4-A90, exhibiting the lowest contact angle value of 69.11° and therefore the highest wettability among the tested conditions; and (c) B6-A30, showing a borderline hydrophobic response with a contact angle of 90.17°.

Table 4. Contact angle values and wettability classifications of titanium surfaces sandblasted under different pressure and angle conditions.

Sample Condition	Contact Angle (°)	Wettability Classification
B2-A30	81.17	Hydrophilic
B2-A60	89.35	Borderline hydrophilic
B2-A90	71.68	Hydrophilic
B4-A30	72.87	Hydrophilic
B4-A60	82.16	Hydrophilic
B4-A90	69.11	Hydrophilic / highest wettability
B6-A30	90.17	Borderline hydrophobic
B6-A60	79.16	Hydrophilic
B6-A90	76.45	Hydrophilic

The lowest contact angle was obtained for B4-A90, although this sample did not exhibit the highest arithmetical mean height, S_a. This behavior may be associated with the formation of crater-like surface depressions under perpendicular particle impact, which can promote local liquid retention and facilitate spreading of the water droplet over the modified titanium surface. On the other hand, B6-A30 showed a borderline hydrophobic response despite its relatively high roughness. This result may be related to the formation of plowing-induced surface channels and possible air retention effects, which can partially restrict droplet spreading on the surface. According to the general contact angle criterion, surfaces with contact angle values below 90° are considered hydrophilic, whereas values slightly above 90° indicate a borderline hydrophobic response. From this perspective, the majority of the sandblasted titanium surfaces can be classified as hydrophilic. For dental implant applications, such hydrophilic behavior is advantageous because it can facilitate the spreading of biological fluids, protein adsorption, and early-stage cell attachment. Although B4-A90 exhibited the highest wettability, B6-A90 provided a more balanced overall surface condition by combining the highest S_a value, complex microcrater morphology, hydrophilic behavior, and enhanced surface hardness, as discussed in the following section.

3.5. Micro-Vickers Hardness Analysis

Micro-Vickers hardness measurements were performed to support the interpretation of sandblasting-induced near-surface plastic deformation and the associated peening effect. The obtained HV_1 values are presented in Table 5. Compared with untreated Pure Ti, all sandblasted samples exhibited higher hardness values, confirming that particle impact induced surface hardening to varying degrees. However, the hardness variation was not strictly linear with sandblasting pressure or angle, suggesting that the indentation response was also affected by local surface morphology, crater distribution, and plowing-induced deformation. Among all tested conditions, B6-A90 exhibited the highest hardness value of 239.5 HV_1. This result supports the interpretation that high-pressure particle impact at a perpendicular angle produced a more pronounced near-surface hardening effect. In contrast, B2-A90 showed the lowest hardness value among the sandblasted samples, which is consistent with its relatively lower roughness and topographic amplitude. Overall, the micro-Vickers hardness results provide additional evidence for the peening-related surface modification effect induced by sandblasting, particularly under high-pressure conditions.

Table 5. Micro-Vickers hardness values of untreated and sandblasted titanium surfaces.

Sample Code	Micro-Vickers Hardness, HV_1
Pure Ti	190.0
B2-A30	214.9
B2-A60	211.2
B2-A90	207.3
B4-A30	229.1
B4-A60	229.4
B4-A90	228.5
B6-A30	234.9
B6-A60	226.1
B6-A90	239.5

Note: Values represent the mean of representative stable indentations. Non-representative indentations affected by local surface irregularities were excluded.

4. Conclusions

The XRD results confirmed that the sandblasting process did not alter the characteristic HCP α-Ti phase structure of Grade 2 titanium, and no additional crystalline phases or crystallographically detectable Al_2O_3 residues were observed. The slight changes in peak intensity and broadening were attributed to near-surface plastic deformation and microstructural disorder caused by particle impact, which was further supported by the micro-Vickers hardness results.

SEM and profilometry analyses demonstrated that the surface modification mechanism changed from plowing-dominated deformation at lower blasting angles to impact-dominated crater formation at higher angles. Sandblasting increased the surface roughness compared with untreated Pure Ti, and B6-A90 exhibited the highest Sa value of 2.58 µm, corresponding to an approximately 200% increase relative to Pure Ti (0.86 µm). The balanced Sp/Sv distribution and complex microcrater morphology of B6-A90 indicate a favorable surface structure for mechanical interlocking.

Contact angle measurements showed that most sandblasted surfaces exhibited hydrophilic behavior. B4-A90 showed the lowest contact angle value of 69.11°, indicating the highest wettability among the tested conditions, whereas B6-A30 exhibited a borderline hydrophobic response with a contact angle of 90.17°. These findings indicate that wettability is governed not only by average roughness but also by crater geometry, surface depression characteristics, and local liquid retention behavior.

Micro-Vickers hardness measurements further confirmed that sandblasting produced a near-surface hardening effect compared with untreated Pure Ti. The highest hardness value was obtained for B6-A90, supporting the interpretation that high-pressure perpendicular particle impact promoted a more pronounced peening-related hardening effect. Overall, B6-A90 was determined as the most favorable surface modification condition because it combined the highest roughness, complex microcrater morphology, hydrophilic behavior, and the highest micro-Vickers hardness response. For dental implant manufacturers, the B6-A90 condition can be considered a practical surface preparation parameter when a rough, mechanically stable, and hydrophilic titanium surface is targeted. Future studies should quantitatively determine the residual stress state of the modified surfaces to further clarify the relationship between sandblasting parameters and subsurface deformation.

Declaration of Ethical Standards

The authors declare that they comply with all ethical standards. This study was conducted only on commercially pure titanium samples and did not involve human participants, animal experiments, biological tissues, or clinical data. Therefore, ethical committee approval was not required.

Credit Authorship Contribution Statement

Author-1: Conceptualization, investigation, methodology and software, visualization and writing – original draft.

Declaration of Competing Interest

The authors have no conflicts of interest to declare regarding the content of this article.

Data Availability Statement

All data generated or analyzed during this study are included in this published article.

5. References

Akbas, O., Reck, L., Jahn, A., Hermsdorf, J., Stiesch, M. & Greuling, A. 2025. Effect of different sandblasting parameters on the properties of additively manufactured and machined titanium surfaces. *In Vivo*, 39 (3), 1767-1785.

Anbarzadeh, E. & Mohammadi, B. 2023. Investigation of the effects of sandblasting, acid etching, and anodizing parameters in the SLA+ anodizing on the surface treatment of titanium dental implant fixtures. *Physics of Metals and Metallography*, 124 (13), 1606-1619.

Ban, S., Iwaya, Y., Kono, H. & Sato, H. 2006. Surface modification of titanium by etching in concentrated sulfuric acid. *Dental materials*, 22 (12), 1115-1120.

Chrcanovic, B., Kisch, J., Albrektsson, T. & Wennerberg, A. 2016. Factors influencing early dental implant failures. *Journal of dental research*, 95 (9), 995-1002.

Elias, C. N., Oshida, Y., Lima, J. H. C. & Muller, C. A. 2008. Relationship between surface properties (roughness, wettability and morphology) of titanium and dental implant removal torque. *Journal of the mechanical behavior of biomedical materials*, 1 (3), 234-242.

Ghara, T., Paul, S. & Bandyopadhyay, P. 2021. Effect of grit blasting parameters on surface and near-surface properties of different metal alloys. *Journal of Thermal Spray Technology*, 30 (1), 251-269.

Gil, F. J., Planell, J. A., Padrós, A. & Aparicio, C. 2007. The effect of shot blasting and heat treatment on the fatigue behavior of titanium for dental implant applications. *Dental Materials*, 23 (4), 486-491.

Gittens, R. A., Scheideler, L., Rupp, F., Hyzy, S. L., Geis-Gerstorfer, J., Schwartz, Z. & Boyan, B. D. 2014. A review on the wettability of dental implant surfaces II: Biological and clinical aspects. *Acta biomaterialia*, 10 (7), 2907-2918.

Khan, A. A., Al Kheraif, A. A., Alhijji, S. M. & Matinlinna, J. P. 2016. Effect of grit-blasting air pressure on adhesion strength of resin to titanium. *International Journal of Adhesion and Adhesives*, 65, 41-46.

Kırman, M., Dikici, T. & Doğan, H. 2023. Dental implantlar için farklı yüzey modifikasyon tekniklerinin titanyumun yüzey özelliklerine etkilerinin karşılaştırılması. *Dicle Üniversitesi Mühendislik Fakültesi Mühendislik Dergisi*, 14 (3), 449-454.

Le Guéhennec, L., Soueidan, A., Layrolle, P. & Amouriq, Y. 2007. Surface treatments of titanium dental implants for rapid osseointegration. *Dental materials*, 23 (7), 844-854.

Liu, T. L., Chen, Z. & Kim, C.-J. 2015. A dynamic Cassie–Baxter model. *Soft Matter*, 11 (8), 1589-1596.

Low, J., Dai, B., Tong, T., Jiang, C. & Yu, J. 2019. In situ irradiated X-ray photoelectron spectroscopy investigation on a direct Z-scheme TiO2/CdS composite film photocatalyst. *Advanced Materials*, 31 (6), 1802981.

Rønold, H. J., Lyngstadaas, S. P. & Ellingsen, J. E. 2003. A study on the effect of dual blasting with TiO2 on titanium implant surfaces on functional attachment in bone. *Journal of Biomedical Materials Research Part A: An Official Journal of The Society for Biomaterials, The Japanese Society for Biomaterials, and The Australian Society for Biomaterials and the Korean Society for Biomaterials*, 67 (2), 524-530.

Rupp, F., Scheideler, L., Olshanska, N., De Wild, M., Wieland, M. & Geis-Gerstorfer, J. 2006. Enhancing surface free energy and hydrophilicity through chemical modification of microstructured titanium implant surfaces. *Journal of Biomedical Materials Research Part A: An Official Journal of The Society for Biomaterials, The Japanese Society for Biomaterials, and The Australian Society for Biomaterials and the Korean Society for Biomaterials*, 76 (2), 323-334.

Sushil, K., Ramkumar, J. & Chandraprakash, C. 2025. Surface roughness analysis: A comprehensive review of measurement techniques, methodologies, and modeling. *Journal of Micromanufacturing*, 25165984241305225.

Sykaras, N., Iacopino, A. M., Marker, V. A., Triplett, R. G. & Woody, R. D. 2000. Implant materials, designs, and surface topographies: their effect on osseointegration. A literature review. *International Journal of Oral & Maxillofacial Implants*, 15 (5).

Thakur, A., Kumar, A., Kaya, S., Marzouki, R., Zhang, F. & Guo, L. 2022. Recent advancements in surface modification, characterization and functionalization for enhancing the biocompatibility and corrosion resistance of biomedical implants. *Coatings*, 12 (10), 1459.

Webb, H. K., Truong, V. K., Hasan, J., Fluke, C., Crawford, R. J. & Ivanova, E. P. 2012. Roughness parameters for standard description of surface nanoarchitecture. *Scanning*, 34 (4), 257-263.

Wennerberg, A. & Albrektsson, T. 2009. Effects of titanium surface topography on bone integration: a systematic review. *Clinical oral implants research*, 20, 172-184.